Proceedings of the ASME 2019 38th International Conference on Ocean, Offshore and Arctic Engineering
OMAE2019
June 9-14, 2019, Glasgow, Scotland, UK

OMAE2019-96686

STRUCTURAL SAFETY ASSESSMENT OF MARINE OPERATIONS FROM A LONG-TERM PERSPECTIVE: A CASE STUDY OF OFFSHORE WIND TURBINE BLADE INSTALLATION

Amrit Shankar Verma*
NTNU
Department of Marine Technology
Trondheim, Norway
Email: amrit.s.verma@ntnu.no

Zhen Gao
NTNU
Department of Marine Technology
Trondheim, Norway
Email: zhen.gao@ntnu.no

Zhiyu Jiang
University of Adger
Department of Engineering Sciences
Grimstad, Norway
Email: zhiyu.jiang@uia.no

Zhengru Ren
NTNU
Department of Marine Technology
Trondheim, Norway
Email: zhengru.ren@ntnu.no

Nils Petter Vedvik
NTNU
Department of Mechanical engineering
Trondheim, Norway
Email: nils.p.vedvik@ntnu.no

ABSTRACT

A marine operation is a complex non-routine activity of limited duration carried out in offshore environment. Due to safety reasons, these operations are normally performed within specific sea state limits, which are derived from numerical modelling and analysis of hazardous events. In view of the uncertainties in the assessment of structural responses under stochastic environmental conditions, these limiting curves correspond to a target structural failure probability recommended in offshore standards (for example, 10^{-4} *per operation as specified by DNV-GL). However, one of the main limitations is that these curves do not reflect site-specific safety assessment. The current paper presents a novel methodology for assessing the structural safety level of marine operations from a long-term perspective. The methodology includes estimation of extreme response distribution under all possible operational sea states (i.e. the operational domain under the limiting sea states) for a given offshore site and is compared to the response limit to obtain an average failure probability. A case study is also presented for a blade root mating process onto preassembled hub using a jack-up crane vessel and risk of impact between root and hub is considered critical. Global time-domain simulations are performed using multibody dynamics, and extreme value distributions for impact velocities are derived for different wind-wave conditions. The allowable impact velocity between the blade root and the hub is determined by an explicit finite element analysis of the damage at the blade root. Finally, the average failure probabilities considering the operational domain are obtained for four different European offshore sites and are compared to the target level of structural failure probability considered for the limiting sea states.*

INTRODUCTION

A marine operation is a complex non-routine activity of limited duration carried out in an offshore environment during the temporary stages of an offshore project [1,2]. It refers to different activities, for example, transportation and assembly of sensitive structural components such as blades of an offshore wind turbine, (Fig. 1(a)), oil and gas production topsides, installation of subsea components, access to offshore platforms with a supply vessel, pipelaying operation (Fig. 1(b)), and towing operations

*Address all correspondence to this author.

(a) (b) (c)

FIGURE 1: Examples of different marine operations [3–5]

(Fig. 1(c)), to name a few. All these activities vary by the nature of their tasks, however, share the same stigma of having a highly complicated and non-linear system where dynamic installation systems, detailed operational procedures, and stochastic environmental conditions interact with human participation for success [6].

Given the complexity of these tasks, the planning phase of a marine operation is of vital importance, and hence risk management study is perfomed. As a part of this study, critical and hazardous events that have the potential to cause failure of the task are identified, and the operational limits that avoid these failures and enable safe installation are determined [7]. It is recommended to express the operational limits in terms of allowable sea state parameters (H_s, T_p, U_w), as the operators can decide the commencement of a task by checking the weather forecast. In general, the limiting sea states are based on experiences, for example, a typical lifting operation in the hydrocarbon industry is performed till $H_s \leq 2m$ [1]. This causes high installation costs, yet it is still acceptable for the hydrocarbon sector given that the project has a high profitability margin and includes less lifting activities. However, for offshore wind turbine industry, experiential based sea state limits are not an ideal choice as there are many lifting tasks and the project has a narrow profitability perimeter. Recent studies [7–9] emphasise the use of response based methods, where the allowable sea states are derived scientifically using numerical models and simulations rather than based on experiences. Acero et. al [7] proposed a generic procedure for estimating response based limiting sea states for planning installation activities. The hazardous events that can cause failure are numerically modelled, and limiting sea states are derived by comparing characteristic extreme responses with allowable values. Only those sea states are considered acceptable for which the characteristic responses are less than allowable values.

Note that the above mentioned characteristic extreme responses are estimated from extreme value distributions, and they correspond to the target safety levels or exceedance probability recommended in offshore stanadrds. These values in general depend upon the nature of installation task and the conseqence of failure events [7]. For example, the target safety percentile for the failure of the lifting wire during the offshore crane operation is considered 10^{-4} [10]. This is because such failure events can be catastrophic and irreversible, and may cause immense loss to the installation task. DNV-GL [10] guidelines further recommend that the installation tasks must be planned such that the target structure failure probability for an installation system is less than 10^{-4} per operation. In total, for all combinations of sea states, a limiting curve for the allowable sea state is obtained and the installation activity is carried out within these limits. Note that the installation activity along this curve corresponds to a constant level of structural failure probability.

One of the main limitations for the above obtained allowable sea state curve is that it lacks the site-specific information i.e. the long-term weather characteristics for an offshore site during the installation tasks are not considered. Thus, the limiting curve refers only to the short-term responses calculated for the reference duration of the installation task, for which the sea state parameters are assumed stationary. A site specific safety assessment approach is necessary to obtain an average failure probability for planning the installation task more efficiently. The present paper proposes a novel methodology based on a long-term approach, where the long-term extreme response distribution for the critical event is obtained as a weighted sum of short-term responses under all possible operational sea states (i.e. the operational domain under the limiting sea state curve). Note that the weights are the probabilities of occurrence of the operational sea states at an offshore site. The current paper also presents a case study for the wind turbine blade mating process onto the preassembled hub, considering the impact loads between a guide

pin and hub. The structural safety assessment is calculated using the proposed methodology and the average failure probability is compared for four different European offshore sites.

METHODOLOGY

All sea state approach

The proposed methodology in this paper is a modified form of the 'all sea state' [11, 12] approach, and therefore a brief overview of the original method is given here. This method was first introduced in late 1950s and is used extensively today in the design of an offshore structure to estimate extreme responses under environmental loads. Given that a permanent offshore structure has a design life of 20-25 years, the method considers response contributions for all possible sea states. In other words, long term extreme response distribution is obtained by combining the conditional extreme responses with long term weather statistics for all realizable environmental conditions $(h,t,w \in \mu)$ [13]. This is expressed mathematically by the relation:

$$F_X^{LT}(x) = \iiint_{\mu} F_{X_r|U_w H_s T_p}^{ST}(x|w,h,t) f_{U_w H_s T_p}(w,h,t)\, dh\, dt\, dw \quad (1)$$

where, $F_X^{LT}(x)$ is the long-term distribution of the extreme responses, μ is the domain of integration and consists of all possible combinations of h,t,and w (see fig. 2) for an offshore site, $F_{X_r|U_w H_s T_p}^{ST}$ is the short-term or conditional distribution of extreme responses for given weather characteristics, and finally $f_{U_w H_s T_p}(w,h,t)$ is the long term weather statistic or the joint probability distribution function of H_s, T_p and U_w for a given offshore site. This distribution is given by the relation:

$$f_{U_w H_s T_p}(w,h,t) = f_{U_w}(w) \cdot f_{H_s|U_w}(h|w) \cdot f_{T_p|U_w,H_s}(t|w,h) \quad (2)$$

where $f_{U_w}(w)$ is the marginal distribution for mean wind speed, which fits the two-parameter weibull distribution given by:

$$f_{U_w}(w) = \frac{\alpha_u}{\beta_u}\left(\frac{w}{\beta_u}\right)^{\alpha_u - 1} \cdot exp\left[-\left(\frac{w}{\beta_u}\right)^{\alpha_u}\right] \quad (3)$$

where α_u and β_u are shape and scale parameters. Again, $f_{H_s|U_w}(h|w)$ is the conditional density function of H_s for given Uw, and fits the two-parameter weibull distribution defined by:

$$f_{H_s|U_w}(h|w) = \frac{\alpha_{HC}}{\beta_{HC}}\left(\frac{h}{\beta_{HC}}\right)^{\alpha_{HC} - 1} \cdot exp\left[-\left(\frac{h}{\beta_{HC}}\right)^{\alpha_{HC}}\right] \quad (4)$$

where α_{HC} and β_{HC} are fuctions of w and are defined as shape and scale parameters respectively. The $f_{T_p|U_w,H_s}(t|w,h)$ is the conditional distibution of T_p given H_s and U_w and fits a lognormal distribution. This is given as:

$$f_{T_p|U_w,H_s}(t|w,h) = \frac{1}{\sqrt{2\pi}\sigma_{ln(T_p)} t} \cdot exp\left[-\frac{1}{2}\left(\frac{ln(t) - \mu_{ln(T_p)}}{\sigma_{ln(T_p)}}\right)^2\right] \quad (5)$$

where $\sigma_{ln(T_p)}$ and $\mu_{ln(T_p)}$ are parameters of lognormal distributions and are also functions of w . It is to be further noted that for the domain μ, the area under the joint distribution curve must be unity. This is given by:

$$\iiint_{\mu} f_{U_w H_s T_p}(w,h,t)\, dh dt dw = 1 \quad (6)$$

Modified all sea state approach

The methodology for obtaining the average failure probability for the installation task is explained here. Given that the installation task is a temporary activity, the domain of integration for long term response evaluation is reduced from all possible sea states $(h,t,w \in \mu)$ to all possible operational limiting sea states (say $h,t,w \in \Omega$); i.e., the domain lying below the limiting sea state curve; see Fig. 2. Therefore, the primary step for this method is to derive the limiting sea state curve and obtain the domain of integration (Ω) using the usual response based approach.

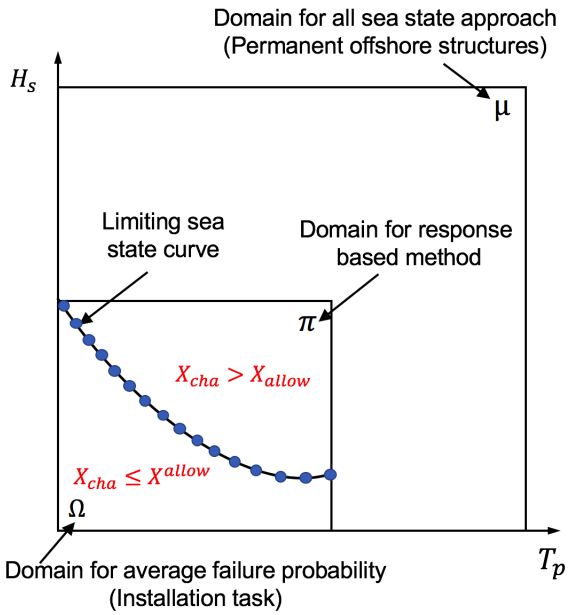

FIGURE 2: Domain of integration for long term approaches

In order to obtain the domain of integration (Ω), an initial operational domain (π) of environmental conditions is chosen for performing response based assessment (see Fig. 2). This domain corresponds to the maximum range of viable sea states for which the installation task can be performed. Any task above this domain is expected to give very large responses and thus should be avoided. For example, the range of U_w for performing a high air lifting activity using crane vessels lies between 2 m/s to 14 m/s. However, for an offshore site, there is still a possibility of having $U_w \geq 20$ m/s, and therefore these U_w must not be considered.

Let us denote this initial operational domain as π (see Fig. 2). Then, $\forall\, h,t,w \in \pi$, response analysis of the installation system characterising the critical event is performed. For each sea state, the conditional distribution of short term extreme responses are established and for a target safety level, characteristic extreme responses (X_{char}) are determined. Finally, only those sea states are acceptable ($\forall\, h,t,w \in \Omega$) for which $X_{char} \leq X_{allow}$, otherwise the sea states are not acceptable. Note that X_{allow} is the allowable limit of the responses, such as, maximum allowable roll motion, maximum impact velocity. All sea states satisfying $X_{char} \leq X_{allow}$ belong to the domain Ω for which the average failure probability is determined. The long term extreme response distribution for the installation task is given by:

$$F_X^{LT}(x) = \frac{\iiint\limits_{\Omega} F^{ST}_{X_r|U_wH_sT_p}(x|w,h,t)\, f_{U_wH_sT_p}(w,h,t)\, dh\, dt\, dw}{\iiint\limits_{\Omega} f_{U_wH_sT_p}(w,h,t)\, dh\, dt\, dw} \quad (7)$$

where all the terms have their usual meaning as in eq. (1) except Ω which is the domain of integration here. Note that the denominator of equation (7) consists of joint distribution of sea state parameters with Ω as the domain of integration. This value corresponds to the average sense and normalises the value of long term response distribution.

Finally, the average failure probability ($P_T^{LT}(T)$) for the installation task is defined as:

$$P_T^{LT}(T) = \int\limits_{X>X_{allow}} f_X^{LT}(x)dx \quad (8)$$

where, X_{allow} is the limiting value of the responses, and $f_X^{LT}(x)$ is the probability density function of long term extreme responses .

CASE STUDY: OFFSHORE WIND TURBINE BLADE MATING PROCESS

A case study for the offshore wind turbine blade mating process onto the preassembled hub using a jack up crane vessel is presented in Fig. 3(a). For a given critical event, the structural safety assessment of the mating task is evaluated and the average failure probability is compared for four different offshore sites.

Critical event

The wind turbine blade mating process is a substantially demanding task, and calls for high precision [16–20]. The blade is lifted from the deck using a crane, and several bolted connections along with the guide pin at the root are mated with the flange holes of the preassembled hub (Fig. 3(b)). The final alignment phase exhibits high relative responses amid root and hub, due to combined effects of wave-induced monopile motion and wind-induced blade root motion [21]. Therefore, a significant risk of impact exists between the guide pin and hub and is considered as the critical event for the mating task.

The most severe risk is when the guide pin impacts the hub in sideways direction [15,21,22] and this is caused due to relative motion of mating systems in the global-y direction; see Fig. 3(c). This scenario is dominant for the cases where the mating process is exposed to collinear wind and wave conditions [15, 23]. Here, impact velocity between root and hub in global-y direction (V_y^{imp}) is considered as the response parameter for structural failure probability calculations.

Choice of target safety level for the mating task

The target safety level for an installation task depends upon the consequence of the failure events. Here, different failure modes for the blade root impact with the hub and their consequences are discussed:

1. **Minor bend of the guide pin**: The guide pin bends inelastically by a small angle ($\phi < 2^\circ$, see Fig. 4). However, the mating process is still achievable without hoisting the lifted blade back to the deck. The target safety level is substantially high (10^{-1}) and the allowable impact velocity is strict ($V_y^{imp} < 0.2m/s$).
2. **Major bend of guide pin**: The guide pin bends by a large angle ($2^\circ < \phi < 7^\circ$, see Fig. 4) along with its significant plastic deformation. The mating process is halted, and the lifted blade is brought back to the vessel. The damaged guide pin is then replaced with a new one and another mating trial is performed. The target safety level is 10^{-2} and the allowable impact velocity lies in the range of $0.2m/s < V_y^{imp} < 0.8m/s$.
3. **Damage to the root laminate**: The guide pin bends by an angle ($\phi > 7^\circ$, see Fig. 4), and induces delamination cracks at the adjacent root laminate due to impact induced tensile stresses. In such cases, the mating process is substantially delayed and the blade requires inspection along with possibility of major repair works offshore. The target safety level is 10^{-4}, and the allowable impact velocity lies in the range of $V_y^{imp} > 0.8m/s$.

In this paper, we consider the second failure mode for structural safety assessment, given that it has acceptable consequences during installation. A target safety level of 10^{-2} along with $V_y^{allow} = 0.76m/s$ are used for estimating the characteristic ex-

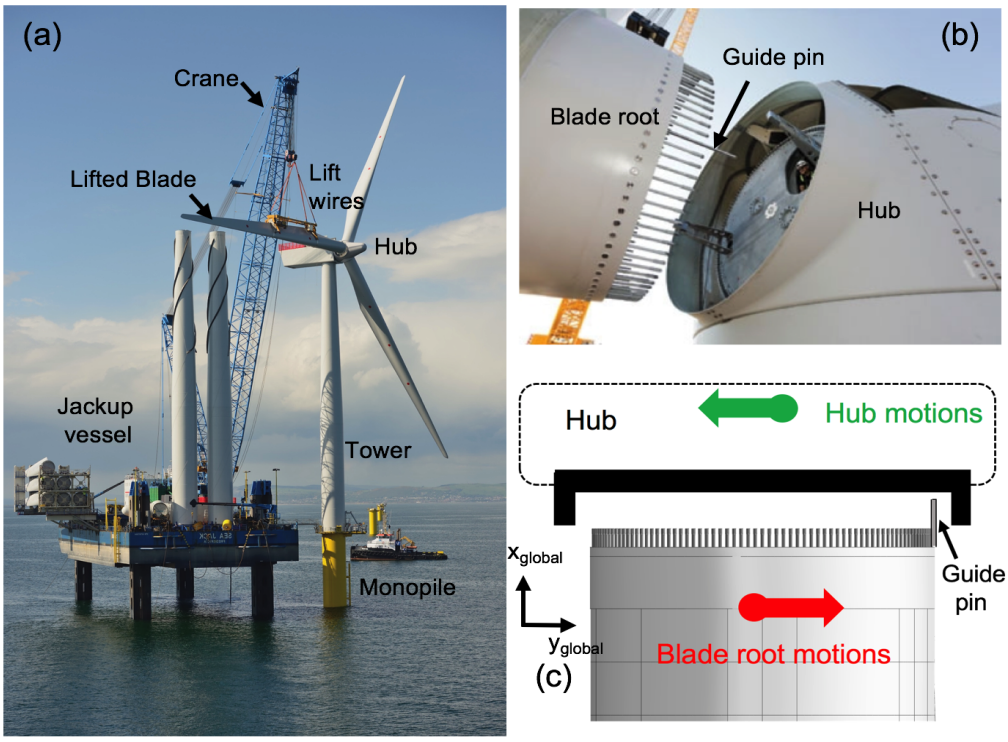

FIGURE 3: (a) Offshore wind turbine blade mating process [3] (b) final alignment phase [14] (c) sideways impact scenario [15]

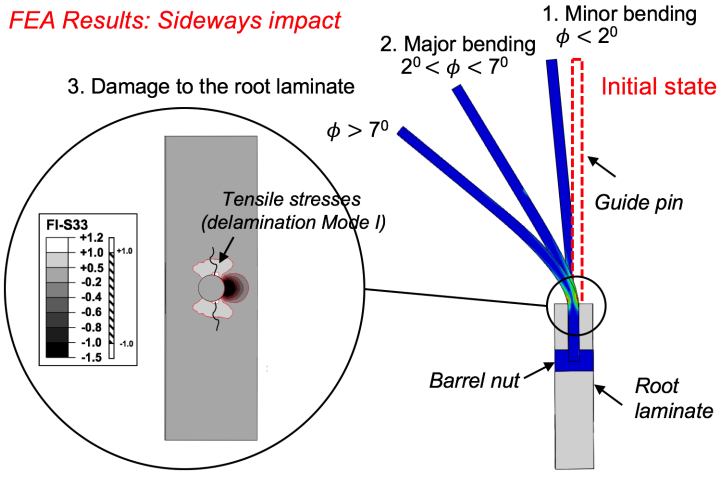

FIGURE 4: Impact-induced failure modes at the blade root [15]

treme responses. Note that these reported values of V_y^{imp} correspond to analysis based on DTU 10 MW blade [24] from [15], and thus are design constraints. In practice, these values can be improved by designing the structural system more efficiently, such as, by modifying the structural behaviour of the guide pin.

Analysis procedure

Fig. 5 presents the analysis procedure for estimating the average failure probability of the mating task.

The first step is the numerical modelling of installation system characterising the mating process in HAWC2 code [25]. Time-domain stochastic analysis is performed for different sea states $(h,t,w) \in \pi$. Then, the conditional extreme value distribution for V_y^{imp} are estimated. Further, for a target safety level of 10^{-2}, characteristic extreme responses (V_y^{char}) are obtained.

The second step is the structural analysis of the blade root impact with the hub using finite element analysis in Abaqus/explicit [26], and different failure modes are studied. This has been already accomplished in the previous study [15], and the results for the allowable impact velocity ($V_y^{allow} = 0.76m/s$) were already discussed.

The third step is the calculation of the domain of integration (Ω) for the long-term response evaluation. For all $(h,t,w) \in \pi$, characteristic short-term extreme responses (obtained from step 1) are compared with V_y^{allow}. Only those sea states qualify for Ω for which the relation $V_y^{char} \leq V_y^{allow}$ is satisfied (see Fig. 5).

The final step is the long-term extreme response evaluation of V_y^{imp}. The conditional distribution of extreme responses are combined with joint distribution of sea state parameters described for an offshore site by using eq. (7). Here, the domain of integration is Ω. Finally, eq. (8) is utilised to estimate the

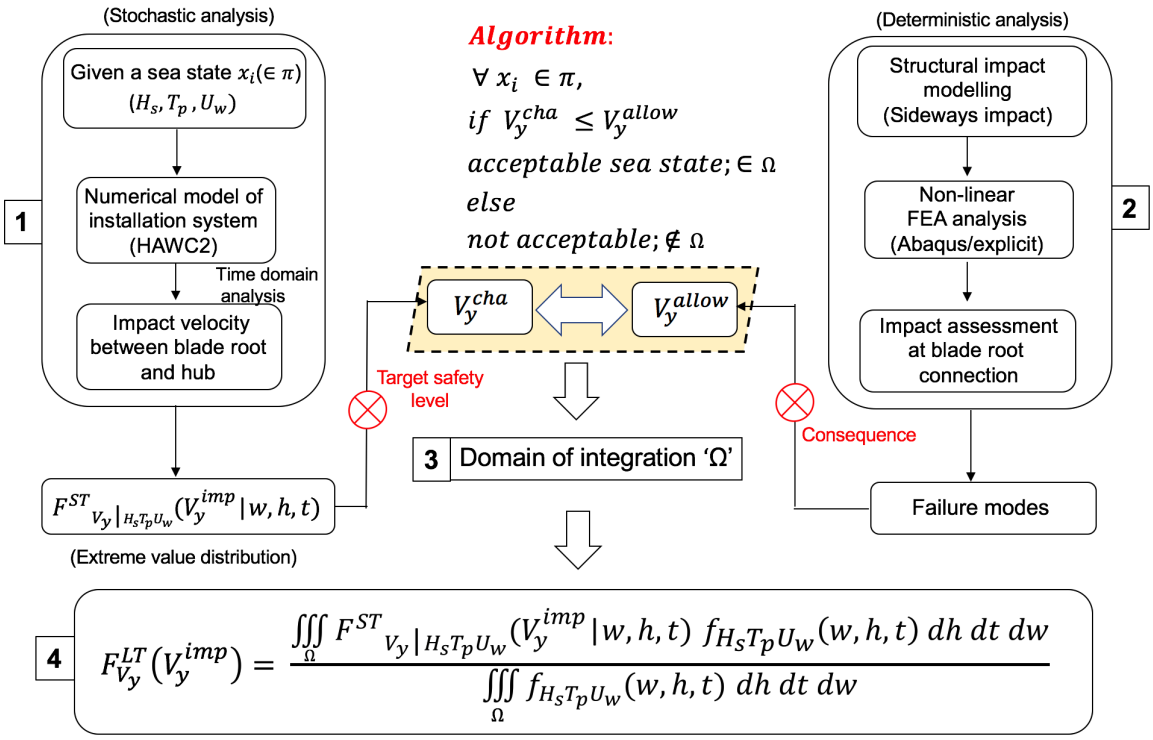

FIGURE 5: Analysis procedure considered for the case study

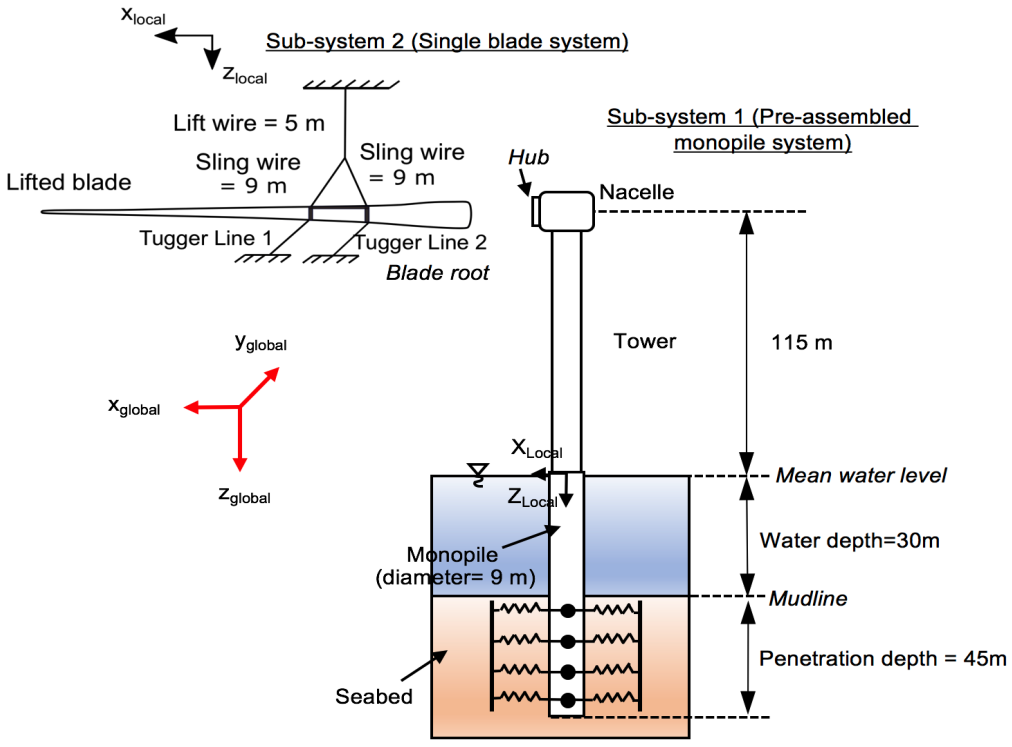

FIGURE 6: Configuration and parameters for the numerical modelling of installation system in HAWC2

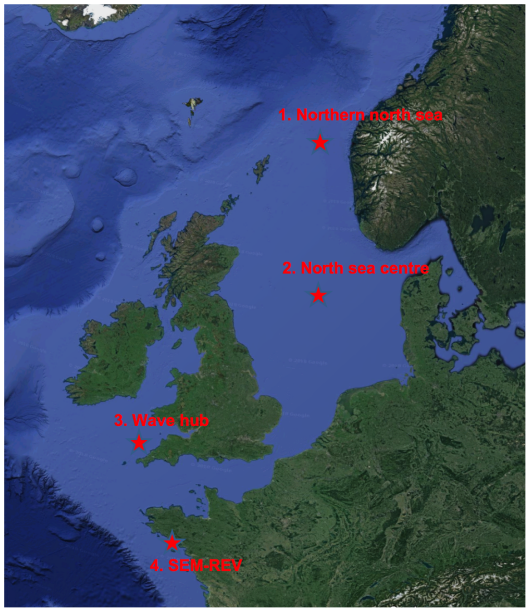

FIGURE 7: Description of offshore sites

average failure probability for four different offshore sites.

Numerical model for global response analysis

The installation system (Fig. 6) is modelled in HAWC2 and consists of (1) monopile sub-sytem and (2) single-blade lift subsystem. All the components of these subsystems are based on reference DTU 10 MW turbine [24].

The monopile subsystem consists of a monopile of diameter 9 m, characterised with Timoshenko beam elaments. The pile-soil interaction effects are defined by $p-y$ curves with soil defined as distributed springs. Other structural components like tower, nacelle, and hub are also modelled with beam elements. Further, wave-induced hydrodynamic loads on the monopile are defined by the Morison's equation [27]. Note that the damping ratio of the monopile is tuned to 1% in the first fore-aft and side-side mode [28], whereas the eigen period of the monopile in the first fore-aft mode is $4.2s$. This implies that any mating operation in the regime of T_p close to $4s$, is expected to give large resonance-induced responses in the fore-aft direction.

The single-blade lift subsystem consists of a blade of length 86.4 m, a yoke, sling wires, lift wires, and tugger lines. The blade is modelled as a single flexible body and is discretised with beam elements. The turbulent field is generated using Mann's turbulence model [29]. The cross flow principle is used along with steady lift and drag coefficients. The tugger lines are 10 m long and are modelled with cable bodies of length 1 m, joined by spherical joints. Note that the jack-up vessel is not considered in the numerical model, and its crane tip is assumed rigidly clamped. This idealisation is valid as their legs are anchored into the seabed during installation providing a steady crane tip.

Details of the selected offshore sites and choice of initial operational domain (π)

Structural safety assessment for the installation task is compared for four different offshore sites- Site (1) Northern north sea; Site (2) North sea centre; Site (3) Wave-Hub, and Site (4) SEM-REV (see Fig. 7). The water depth at these sites are assumed to be same for blade installation using jack-up vessel. The joint distributions for these sites are given by eqs. (2)-(5), and the parameters describing them are obtained from [30, 31] and are also mentioned in Table 1 of Appendix A. An initial choice of operational domain (π) is made for response-based assessment - H_s varies with a step of $0.5m$ in the range $0.5 \leq H_s \leq 3$; T_p varies with a step of $2s$ in the range $2 \leq T_p \leq 16$, and U_w varies with a step of $2m/s$ in the range $2 \leq U_w \leq 14$. Here U_w corresponds to mean wind speed at hub height with turbulence intensity of 0.18. Thus, there are 336 environmental conditions considered, where for each case 20 seeds are analysed. In total, there are 20,160 environmental cases used for time domain analyses. Each analysis is carried out for $1000s$, out of which the initial $400s$ are removed during post processing to evade startup effects.

RESULTS AND DISCUSSION

Impact velocity between blade root and hub (V_y^{imp})

The response parameter of interest in this study is the impact velocity between blade root and hub in the global-y direction (V_y^{imp}). Fig. 8(a) compares the V_y^{imp} for mating operation in the environmental condition corresponding to $H_s = 2.5m$, $U_w = 6m/s$, and two different T_p $(4s, 12s)$. Given that the natural period of the monopile in the first fore-aft mode is $4.2s$, the impact velocity is substantially high for $T_p = 4s$, with maximum value reaching more than 1.5 m/s. Note that this value is greater than the allowable impact velocity ($V_{allow} = 0.76m/s$) utilised in this study for safety assessment. On the other hand, impact velocity for mating operation at $T_p = 12s$, is comparatively less and the maximum value from the time series reaches 0.4 m/s, which is less than the allowable value of 0.76 m/s ($V_{allow} = 0.76m/s$). Fig. 8(b) also compares the spectral density curves for V_y^{imp} for mating operation for the above environmental conditions ($H_s = 2.5m$, $U_w = 6m/s$, and $T_p = 4s$ and $T_p = 12s$). There are two peak frequencies observed in the spectral density curve, one corresponds to the rotational mode of the blade at $0.08Hz$, whereas the other corresponds to the monopile first fore-aft mode at $0.24Hz$. It can be clearly seen that the peak frequency corresponding to the monopile is substantial for $T_p = 4s$ and is reduced for larger T_p ($T_p = 12s$), which is away from the excitation frequency of the monopile. Note that the above discussed results correspond to only one seed for the given environmental condition. In order to perform response statistics and determine short term and long term extreme value distributions, there were 20 seeds analysed for each load case in the chosen initial oper-

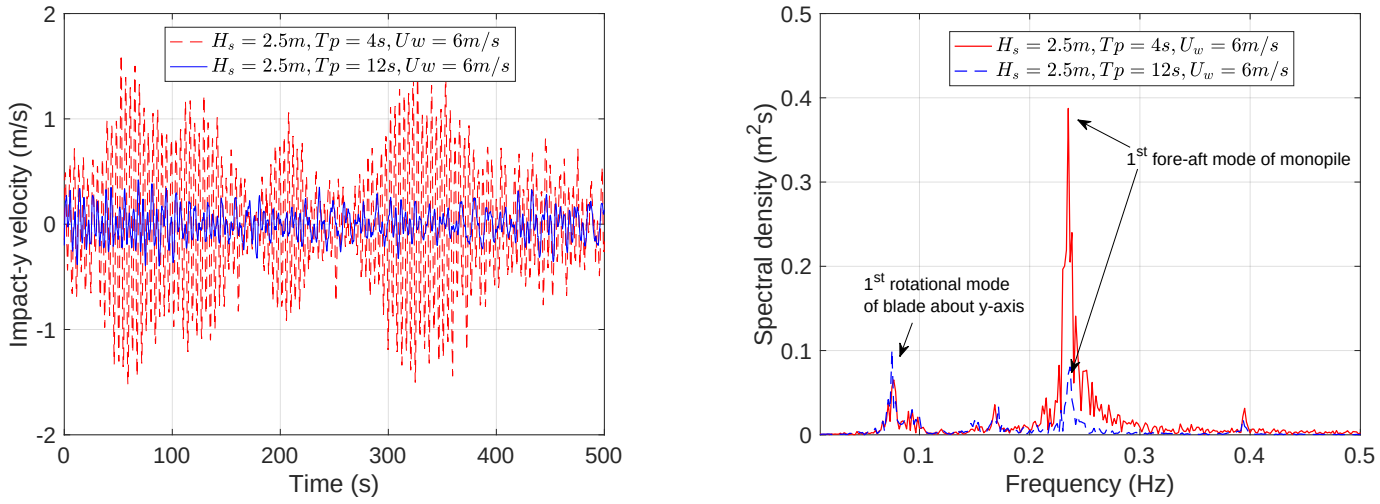

(a) (b)

FIGURE 8: Comparison of V_y^{imp} : (a) Time histories (b) Spectral densities

ational domain π ($h,t,w \in \pi$). This value of 20 seeds was obtained by a statistical convergence study performed in previous work and the details can be found in [15, 23].

Determination of short term conditional distribution of extreme responses $F^{ST}_{V_y|U_wH_sT_p}(V_y^{imp}|w,h,t)$

Here, the conditional extreme value distributions of V_y^{imp} for given wave characteristics are determined. Maximum value of impact velocity is extracted from each time series (20 dots corresponding to each environmental case) and are fitted to gumbel distribution paper (Fig. 9(a)). Once the gumbel fit showed satisfactory results, the parameters of the gumbel distributions are determined. Note that the gumbel distribution has the form $F(V_y^{imp}) = exp(-exp(-(V_y^{imp} - \mu)/\beta))$, where μ and β are location and shape parameters respectively. These parameters are then used to describe the short term conditional distribution of extreme responses for given wave characteristics. Overall, there are 336 sets of gumbel parameters (μ and β) for all 336 combinations of environmental cases ($h,t,w \in \pi$).

Fig. 9(a) shows the gumbel fitting of data points corresponding to V_y^{imp} for five environmental load cases ($H_s = 2.5m$, $U_w = 6m/s$, and $T_p = 4s, 6s, 8s, 10s, 12s$). It can be observed that the data fitted the gumbel plot satisfactorily. Further, the gumbel parameters (μ and β) are determined, and are also mentioned next to the fitted line on the gumbel probability paper in Fig. 8(a). Based on these estimated parameters, the short term conditional distributions ($F^{ST}_{V_y|U_wH_sT_p}(V_y^{imp}|w,h,t)$) are also shown in Fig. 9(b) which correspond to the above discussed environmental cases. Note that the extreme value distribution for $T_p = 4s$, has large extreme values of V_y^{imp}, and thus corresponds to the first distribution on the right side. The extreme values of V_y^{imp} become less for larger values of T_p, and thus the distribution shifts towards the left side with increasing T_p.

Determination of characteristic extreme responses V_y^{char} and finding the domain of integration (Ω)

The target exceedance probability of the allowable impact velocity for root and hub is assumed as 10^{-2} in this work. Note that the allowable impact velocity is considered as 0.76 m/s ($V_{allow} = 0.76m/s$) and is obtained from the finite element study [21]. This value corresponds to the threshold level of impact velocity where the failure mode in the blade root consists of inelastic bending of guide pin, but no damage to the root laminate.

First, the characteristic extreme responses (V_y^{char}) are determined for each of the short term response distributions ($h,t,w \in \pi$), using an exceedence probability of 10^{-2} and then are compared with the V_{allow}. Only those sea states are considered in the domain Ω, which satisfy the relation: $V_y^{char} \leq V_{allow}$. Note that Ω lies below the limiting sea state curve and is used as the domain of integration for the long term response evaluation.

Fig. 9(c) presents the determination of characteristic extreme responses (V_y^{char}) for the five discussed enviromental load cases ($H_s = 2.5m$, $U_w = 6m/s$, and $T_p = 4s, 6s, 8s, 10s, 12s$). The 10^{-2} exceedence level is used to determine the V_y^{char}, and is marked with black circular dots in Fig. 9(c). Each black dot which corresponds to the characterstic extreme value for a given sea state is compared with $V_{allow} = 0.76m/s$. It is found that only $T_p = 10s$, and $T_p = 12s$ for $H_s = 2.5m$ and $U_w = 6m/s$ qualify for the domain Ω, and have characteristic extreme responses

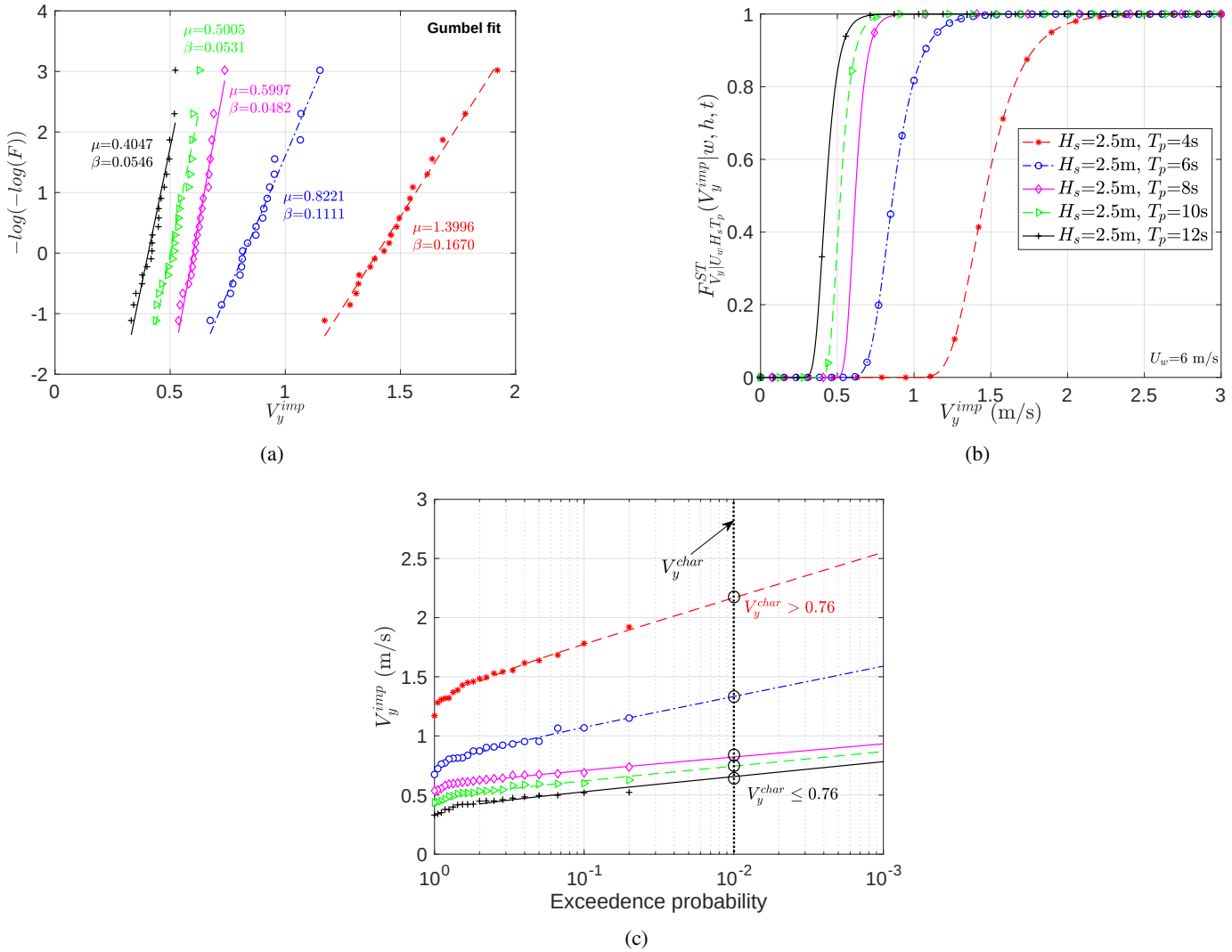

FIGURE 9: (a) Gumbel fitting of raw data (b) Short term extreme response distributions (c) Estimation of characteristic extreme responses

less than 0.76 m/s. Similar investigations are performed for all $h,t.w \in \pi$, and characteristic extreme responses are compared with $V_{allow} = 0.76m/s$ to obtain a complete set of environmental conditions representing the domain of integration Ω. Figs. 10(a)-(c) present the obtained domains of integration in terms of H_s and T_p for three different $U_w = 6, 10, 14m/s$, and are shaded as grey area. Note that all $h,t,w \in \Omega$ satisfy the relation: $V_y^{char} \leq V_{allow}$ and are also marked in the figs. 10(a)-(c).

Determination of long term extreme response distribution ($F_{V_y}^{LT}(V_y^{imp})$) and comparison of average failure probability ($P_T^{LT}(T)$) for four different offshore sites

Once the domain of integration (Ω) is obtained, long term extreme value distributions for V_y^{imp} are calculated for four different European offshore sites. Here, conditional distributions of short term extreme responses are combined with joint probability density function of H_s, T_p, U_w (for offshore sites) by using eq. (7). Finally, the allowable impact velocity ($V_{allow} = 0.76m/s$) is used to determine the average failure probability of the installation task using eq. (8).

Fig. 11(a) compares the long term extreme value distribution of impact velocity ($F_{V_y}^{LT}(V_y^{imp})$) for performing blade mating task at four different offshore sites. It can be clearly seen that these distributions vary for all the four offshore sites, with site 2 (North sea centre) distribution located on the rightmost side. This means that the chances of developing excessive responses during the mating task is highest for site 2 compared to the other offshore sites. On the other hand, site 4 (SEM-REV) is located on the leftmost side and thus has the chance of developing least re-

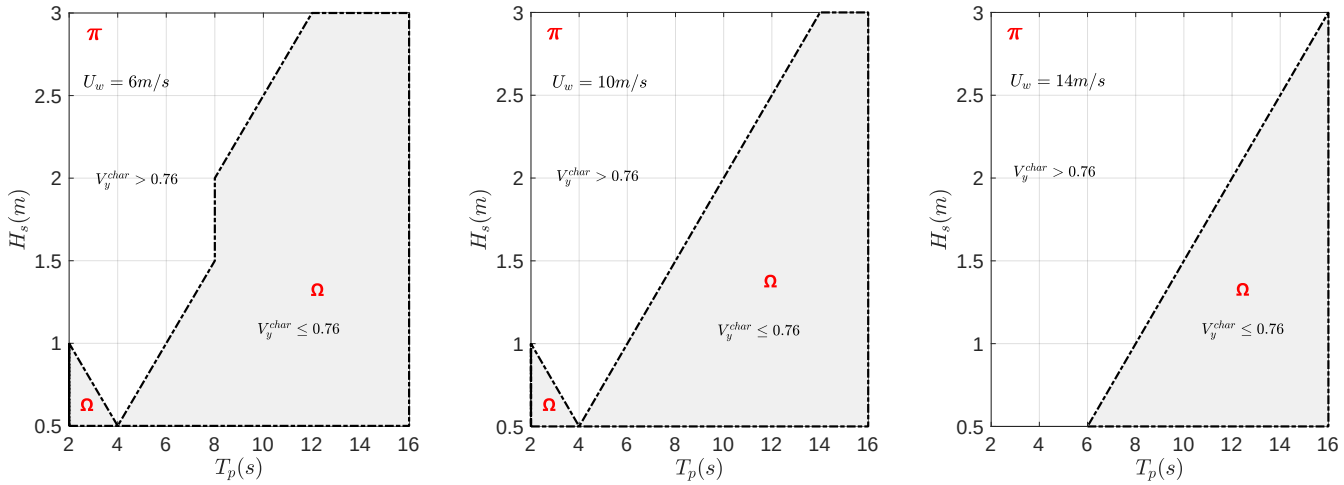

FIGURE 10: Domains of integration (Ω) in terms of H_s and T_p for (a) $U_w = 6m/s$ (b) $U_w = 10m/s$ (c) $U_w = 14m/s$

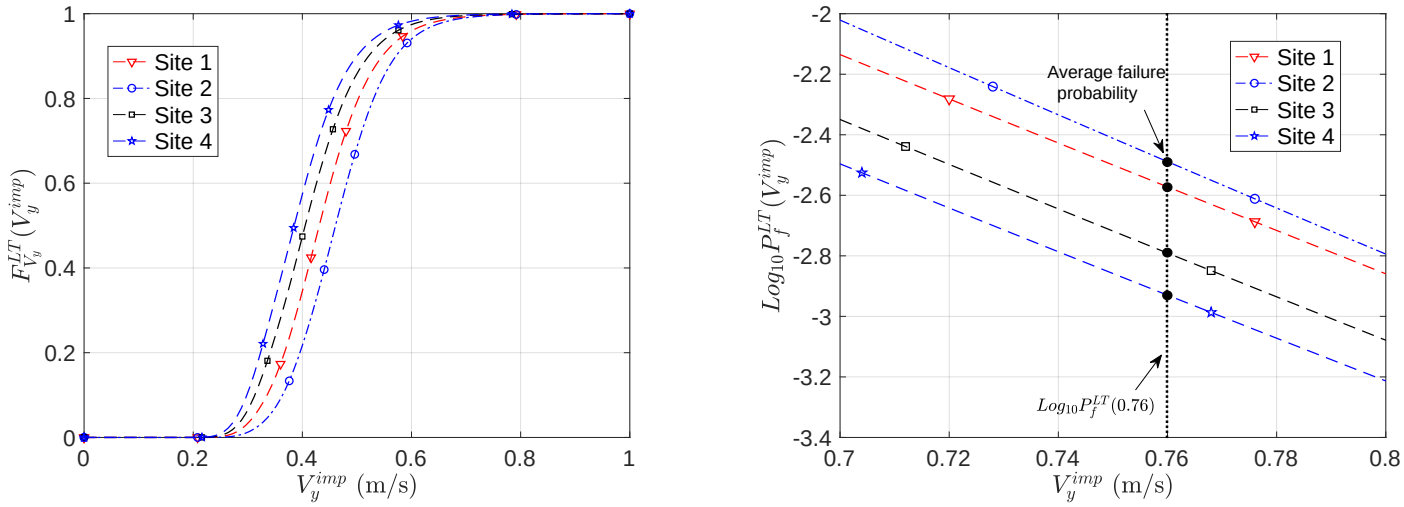

(a) (b)

FIGURE 11: Comparison of (a) Long term extreme response distributions (b) Average failure probability for offshore sites - Site 1: Northern north sea, Site 2: North sea centre, Site 3: Wave-Hub, and Site 4: SEM-REV

sponses compared to the other offshore sites. A similar argument can also be confirmed from Fig. 11(b), where the average failure probability for the blade mating process is compared for four different offshore sites, corresponding to an allowable impact velocity ($V_{allow} = 0.76m/s$). It is clearly observed that the average failure probability for peforming blade mating task is highest for Site 2 ($10^{-2.5}$), and least for Site 4 ($10^{-2.95}$). Note that the average failure probability for performing the installation task for all the offshore sites are less than (10^{-2}) at $V_{allow} = 0.76m/s$. Hence, this implies that the response based method overstimates the safe operational domain (Ω) for planning the installation task given that the average failure probability is less than the target exceedence level.

CONCLUSION AND FUTURE WORK

The present paper proposed a novel methodology for performing the structural safety assessment of marine operations from a long term perspective. The methodology is a modified form of 'all sea state approach' and utilises the area under the

limiting sea state curve as the domain of integration. A case study was also presented for the offshore wind turbine blade mating task on the preassembled hub, where the impact between the guide pin and hub in the sideways direction was considered critical. Failure modes and consequences were categorised, and a target safety level of 10^{-2} was chosen to obtain characteristic extreme responses. Time domain analyses for a chosen initial operational domain were performed and long term extreme response distributions and average failure probability were compared for four different offshore sites. It was found that the averge failure probabilities varies for different sites and is less than the target safety level used for estimating characteristic responses. Overall, the limiting sea states obtained from response based method are conservative. Future study will emphasise on expanding the limiting sea states by optimising the domain of integration so that the average failure probability for an installation task at an offshore site corresponds to the prescribed target safety level.

ACKNOWLEDGMENT

The authors are grateful to SFI MOVE projects supported by the Research Council of Norway, NFR project number 237929.

REFERENCES

[1] Acero, W. I. G., 2016. "Assessment of Marine Operations for Offshore Wind Turbine Installation with Emphasis on Response-Based Operational Limits". PhD Thesis, NTNU.

[2] DNV-GL, 2016. "Marine operations and marine warranty". *Offshore Standard*.

[3] www.siemens.co.uk/en/newspress/index. Picture taken.

[4] http://www.hmc.nl/portfolio/zhong-ren-3-with spar/. Picture taken.

[5] http://www.saipem.com. Picture taken.

[6] Gao, Z., Wilson Guachamin Acero, L. L., Zhao, Y., Li, C., and Moan, T., 2016. "Numerical simulation of marine operations and prediction of operability using response-based criteria with an application to installation of offshore wind turbine support structures". In Marine Operations Specialty Symposium (MOSS 2016).

[7] Acero, W. G., Li, L., Gao, Z., and Moan, T., 2016. "Methodology for assessment of the operational limits and operability of marine operations". *Ocean Engineering,* ***125***, pp. 308–327.

[8] Li, L., Acero, W. G., Gao, Z., and Moan, T., 2016. "Assessment of allowable sea states during installation of offshore wind turbine monopiles with shallow penetration in the seabed". *Journal of Offshore Mechanics and Arctic Engineering,* ***138***(4), p. 041902.

[9] Gintautas, T., and Sørensen, J. D., 2017. "Improved methodology of weather window prediction for offshore operations based on probabilities of operation failure". *Journal of Marine Science and Engineering,* ***5***(2), p. 20.

[10] DNV, 2014. "DNV-OS-H205–Lifting operations Part 2-5". *Offshore Standard*.

[11] Jasper, N. H., 1956. "Statistics distridbution patterms of ocean waves and of wave-induced ship stresses and motions". *SNAME,* ***64***.

[12] Li, Q., Michailides, C., Gao, Z., and Moan, T., 2018. "A comparative study of different methods for predicting the long-term extreme structural responses of the combined wind and wave energy concept semisubmersible wind energy and flap-type wave energy converter". *Proceedings of the Institution of Mechanical Engineers, Part M: Journal of Engineering for the Maritime Environment,* ***232***(1), pp. 85–96.

[13] Haver, S., 2017. "Metocean modelling and prediction of extremes". *Lecture notes in TMR4195-Design of Offshore Structures. Department of Marine Technology, Norwegian University of Science and Technology*.

[14] https://www.siemens.com/press/en/events/2012/energy/2012 09-london.php. Picture.

[15] Verma, A. S., Jiang, Z., Vedvik, N. P., Gao, Z., and Ren, Z., 2019. "Impact assessment of a wind turbine blade root during an offshore mating process". *Engineering Structures,* ***180***, pp. 205–222.

[16] Verma, A. S., Vedvik, N. P., and Gao, Z., 2019. "A comprehensive numerical investigation of the impact behaviour of an offshore wind turbine blade due to impact loads during installation". *Ocean Engineering,* ***172***, pp. 127–145.

[17] Verma, A. S., Vedvik, N. P., and Gao, Z., 2017. "Numerical assessment of wind turbine blade damage due to contact/impact with tower during installation". *IOP Conference Series: Materials Science and Engineering,* ***276***, pp. 012–025.

[18] Verma, A. S., Zhao, Y., Gao, Z., and Vedvik, N. P., 2019. "Explicit structural response-based methodology for assessment of operational limits for single blade installation for offshore wind turbines". In Proceedings of the Fourth International Conference in Ocean Engineering (ICOE2018), Springer, pp. 737–750.

[19] Ren, Z., Skjetne, R., Jiang, Z., Gao, Z., and Verma, A. S., 2019. "Integrated gnss/imu hub motion estimator for offshore wind turbine blade installation". *Mechanical Systems and Signal Processing,* ***123***, pp. 222–243.

[20] Verma, A. S., Haselbach, P. U., Vedvik, N. P., and Gao, Z., 2018. "A global-local damage assessment methodology for impact damage on offshore wind turbine blades during lifting operations". In ASME 2018 37th International Conference on Ocean, Offshore and Arctic Engineering, American Society of Mechanical Engineers, pp. V010T09A064–V010T09A064.

[21] Verma, A. S., Jiang, Z., Gao, Z., and Vedvik, N. P. "Effects

[APPENDIX A]: *Table 1*: *Parameters defining the joint density functions for the chosen offshore sites* [30, 31]

Distributions	Parameters	Site1	Site2	Site 3	Site 4
Marginal U_w	α_u	2.05	2.299	2.05	2.262
	β_u	7.859	8.920	7.859	7.635
Conditional H_s given U_w	a_1	2.0	1.755	2.044	1.894
	a_2	0.135	0.184	0.034	0.012
	a_3	1.0	1.000	1.375	1.741
	b_1	1.8	0.534	1.323	0.929
	b_2	0.2	0.070	0.032	0.024
	b_3	1.322	1.435	1.757	1.827
Conditional T_p given U_w and H_s	θ	-0.19	-0.477	-0.233	-0.268
	γ	1	1.000	1.0	1.0
	e_1	4.883	5.563	8.0	5.0
	e_2	2.68	0.798	2.6	5.883
	e_3	0.529	1.000	0.409	0.201
	f_1	1.764	3.5	1.8	2.0
	f_2	3.426	3.592	3.478	3.947
	f_3	0.78	0.735	0.667	0.620
	k_1	-0.0017	0.050	0.002	-0.002
	k_2	0.259	0.388	0.298	0.341
	k_3	-0.113	-0.321	-0.166	-0.186

of a passive-tuned mass damper on blade root impacts during the offshore mating process". *Marine Structures (Under Review)*.

[22] Verma, A. S., Jiang, Z., Ren, Z., Gao, Z., and Vedvik, N. P. "Effects of wind-wave misalignment on a wind turbine blade mating process". *Journal of Marine Science and Applications (Under Review)*.

[23] Jiang, Z., Gao, Z., Ren, Z., Li, Y., and Duan, L., 2018. "A parametric study on the final blade installation process for monopile wind turbines under rough environmental conditions". *Engineering Structures,* ***172***, pp. 1042–1056.

[24] Bak, C., Zahle, F., Bitsche, R., Kim, T., Yde, A., Henriksen, L. C., Hansen, M. H., Blasques, J. P. A. A., Gaunaa, M., and Natarajan, A., 2013. "Description of the DTU 10 MW Reference Wind Turbine". *Danish Wind Power Research 2013*.

[25] Larsen, T. J., and Hansen, A. M., 2007. "How 2 HAWC2, the user's manual".

[26] Hibbitt, H., Karlsson, B., and Sorensen, P., 2016. "Abaqus analysis users manual version 2016".

[27] Morison, J., Johnson, J., Schaaf, S., et al., 1950. "The force exerted by surface waves on piles". *Journal of Petroleum Technology,* ***2***(05), pp. 149–154.

[28] Shirzadeh, R., Devriendt, C., Bidakhvidi, M. A., and Guillaume, P., 2013. "Experimental and computational damping estimation of an offshore wind turbine on a monopile foundation". *Journal of Wind Engineering and Industrial Aerodynamics,* ***120***, pp. 96–106.

[29] Mann, J., 1994. "The spatial structure of neutral atmospheric surface-layer turbulence". *Journal of Fluid Mechanics,* ***273***, pp. 141–168.

[30] Li, L., Gao, Z., and Moan, T., 2015. "Joint distribution of environmental condition at five european offshore sites for design of combined wind and wave energy devices". *Journal of Offshore Mechanics and Arctic Engineering,* ***137***(3), p. 031901.

[31] Johannessen, K., Meling, T. S., Hayer, S., et al., 2001. "Joint distribution for wind and waves in the northern north sea". In The Eleventh International Offshore and Polar Engineering Conference, International Society of Offshore and Polar Engineers.